Temporal and spectral control of single-photon frequency upconversion for pulsed radiation

Xiaorong Gu, Kun Huang, Yao Li, Haifeng Pan, E Wu,[a] and Heping Zeng[a]
State Key Laboratory of Precision Spectroscopy, East China Normal University, Shanghai 200062, People's Republic of China

(Received 13 November 2009; accepted 5 March 2010; published online 31 March 2010)

We demonstrate efficient single-photon detection at 1.04 μm with quite low background counts by using the frequency upconversion detection technique with pulsed single-photon source and strong pump field prepared from two synchronized fiber lasers. Temporal and spectral control of the pump and signal lasers enabled an upconversion efficiency of 81.1%. As the system was pumped at a wavelength longer than that of the signal, the corresponding background counts were reduced down to 1.5×10^3 s^{-1} due to efficient suppression of parametric fluorescence in the periodic poled lithium niobate crystal. © *2010 American Institute of Physics*. [doi:10.1063/1.3374330]

Recent research shows promising applications of nonlinear frequency upconversion in ultrasensitive detection of infrared single photons.[1–3] The infrared single photons are converted to the visible regime by sum frequency generation in a quadratic nonlinear crystal,[4] where silicon avalanche photodiodes (APDs) can be harnessed to avoid low quantum efficiency and repetition rate, high dark counts, and external detection gate of InGaAs APDs. This technique is also useful for ultrasensitive detection of single photons at the wavelength around 1 μm where neither Si-APDs nor InGaAs APDs work with high quantum efficiencies. Single photons around 1 μm can be converted to the visible region with a nearly unity conversion efficiency and thus detected efficiently by using Si-APDs. This may stimulate interesting applications using compact ytterbium-doped fiber or solid-state lasers around 1.04 μm in deep space communication, laser detection and ranging, and medical diagnosis.[5,6] In order to reduce the background counts and especially to suppress the pump-induced parametric fluorescence, the single-photon frequency upconversion should be better driven by pump pulses of longer wavelength than the signal.[7,8] By using an erbium-doped mode-locked fiber laser as the pump source (1.56 μm) to upconvert the infrared photons at 1.06 μm, efficient single-photon frequency upconversion was demonstrated with ultralow background counts.[8] As the signal photons were in continuous-wave mode while the pump pulses came from the mode-locked laser, the low duty-cycle ratio of the mode-locked laser pulses lead to a low overall detection efficiency since most of the signal photons were mainly distributed outside of the pump pulse envelop. In order to improve the single-photon upconversion detection efficiency, the single-photon pulses should be synchronized with the pump pulses to guarantee a synchronously gated frequency upconversion. Efficient frequency upconversion requires precise control of the synchronized signal and pump pulses in the time and spectrum domain.

In this letter, we report on single-photon frequency upconversion detection with high conversion efficiency and low background counts based on two synchronized fiber lasers. The single-photon signal and the escort pump were from an ytterbium-doped fiber laser (YDFL) and erbium-doped fiber laser (EDFL), respectively, ensuring that each single photon could interact with the corresponding pump pulse in a periodic poled lithium niobate (PPLN) crystal. By engineering the spectral bandwidths and temporal durations of both pump and signal pulses, the all-optical synchronization technique and long-wavelength pumping scheme enabled a conversion efficiency of 81.1% with the corresponding background counts of 1.5×10^3 s^{-1}.

The detection scheme used in our experiment is illustrated in Fig. 1. The single-photon frequency upconversion system was composed of two synchronized fiber lasers (for the single-photon and escort pump sources) and the frequency upconversion detection. Two fiber lasers were synchronized in the master-slave synchronization scheme.[9] The master was an EDFL passively mode-locked by nonlinear polarization rotation effects with a repetition rate of 17.6 MHz. In order to get a narrow spectrum for approaching the quasiphase-matching bandwidth of the PPLN crystal (~0.3 nm), a fiber Bragg grating (FBG) was used as a bandpass filter outside of the laser cavity. The FBG reflection was further amplified by an erbium-doped fiber amplifier to reach a maximum power about 59.3 mW, with the spectrum centered at 1.56 μm and full width at half-maximum (FWHM) bandwidth 0.65 nm [Fig. 2(b)]. The FWHM of the amplified

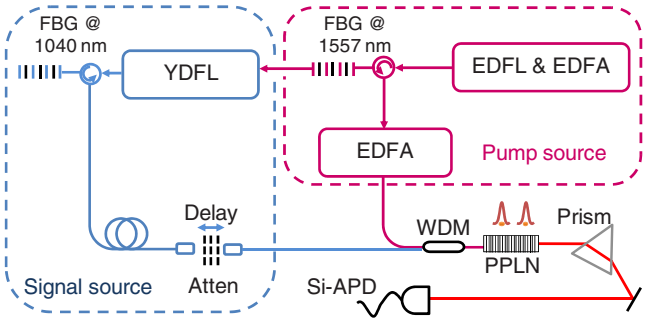

FIG. 1. (Color online) Experimental setup of the synchronous single-photon frequency upconversion detection. EDFL, erbium-doped fiber laser; EDFA, erbium-doped fiber amplifier; YDFL, ytterbium-doped fiber laser; Cir, circulator; FBG, fiber Bragg grating; WDM, wavelength division multiplexer; Col, collimator; Atten, attenuator; PPLN, periodically poled lithium niobate crystal.

[a]Authors to whom correspondence should be addressed. Electronic addresses: ewu@phy.ecnu.edu.cn and hpzeng@phy.ecnu.edu.cn.

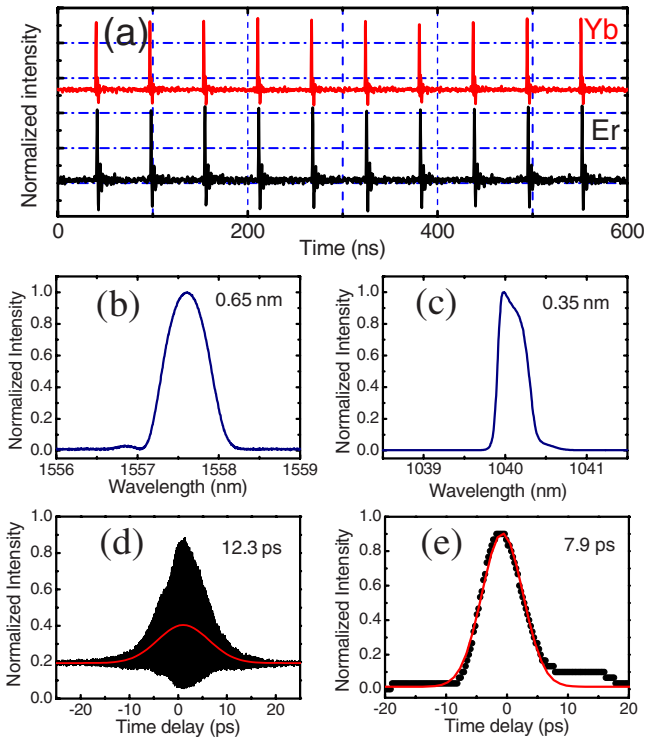

FIG. 2. (Color online) (a) Synchronous pulse trains of the signal (Yb) and the pump (Er) lasers. Spectrum of the pump source from the EDFL (b) and the signal source from the YDFL (c), respectively. Autocorrelation pulse profiles of the pump source from the EDFL (d) and the signal source from the YDFL (e), respectively. Solid symbols are the experimental data and solid curves are the Gaussian fits to the data.

pulse duration was 12.3 ps, as the autocorrelation measurement showed in Fig. 2(d). The transmission from the FBG was used as a trigger by means of cross-phase modulation effect to initiate the mode-locking of a nonlinear polarization rotation mode-locked YDFL (slave laser). A 1.04 μm/1.56 μm wavelength-division multiplexer (WDM) was inserted in the slave cavity for the master injection. Finely tuning the intracavity polarization state and cavity length of the slave laser, synchronization between the EDFL and YDFL was achieved as shown in Fig. 2(a).[9] An additional FBG at 1.04 μm was employed at the output of the slave laser to get a narrow spectrum of the signal photons. The filtered spectrum was centered at 1.04 μm as shown in Fig. 2(c) with the FWHM bandwidth about 0.35 nm, which was appropriate for the sum frequency interaction. Figure 2(e) shows the autocorrelation trace of the slave YDFL pulse after the FBG with the FWHM of 7.9 ps. The timing jitter between the pump source and the single-photon source was measured to be 45 fs from the relevant sum-frequency intensity fluctuation.[10] The low timing jitter profited from the all-optical synchronization technique, where the spectral bandwidths were properly adjusted by FBGs. By engineering the structures and intracavity dispersion-management of the two fiber lasers, the EDFL and followed fiber amplifier generated pump pulses of a little larger pulse duration than the YDFL signal. The single-photon signal could be synchronously gated within the pump pulse, and guarantee efficient synchronous frequency upconversion.

The signal photons at 1.04 μm were combined with the pump pulses at 1.56 μm by a WDM. The mixed beams in

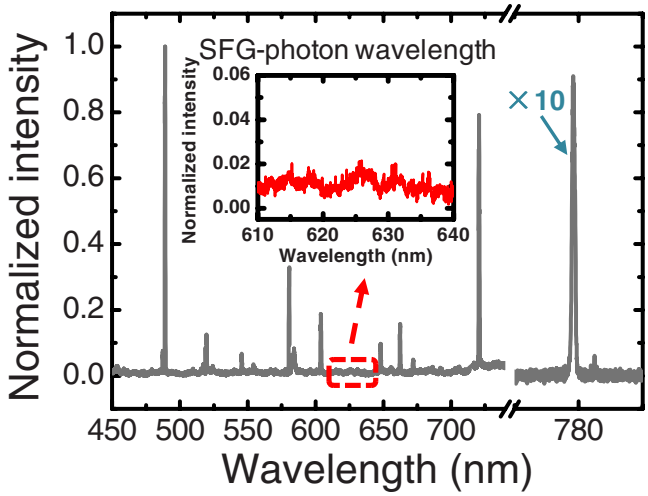

FIG. 3. (Color online) Background spectrum in the visible region without the signal photons injection. Inset: the detailed background spectrum around the SFG-photon wavelength.

fiber were collimated to free space by a collimator and then focused at the center of the PPLN crystal by a lens of 100-mm focal length. The signal and pump beams were controlled to have almost the same the beam waists at the center of the 50-mm-long PPLN crystal. The polarizations of the pump and signal-photon pulses were adjusted independently by two fiber polarization controllers, and enforced to be the same by a Glan prism.

Finely tuning the time delay between the signal and pump pulses to have the temporal overlap, the sum-frequency photons were generated at the center wavelength of 0.62 μm. The operation temperature of the crystal was controlled around 130.4 °C within a fluctuation less than 0.1 °C, which allowed a quasiphase-matching frequency upconversion for the PPLN with a grating period of 11.0 μm.

The signal pulses at 1.04 μm were attenuated to contain 0.11 photons per pulse (1.99×10^{6} s^{-1}) for the upconversion. Before arriving at the Si-APD single-photon counting module (SPCM), the upconverted output photons were steered to pass through a group of spectral and spatial filters. The total transmittance η_T of the combined filters for the sum-frequency photons was about 48.4%. The sensitive SPCM counted the sum-frequency photons with a quantum efficiency η_D of 70% and dark counts around 200 s^{-1}.

We recorded the noise spectrum before the bandpass filter without the signal source (Fig. 3). No observable peaks around the wavelength of the sum-frequency photons appeared as shown in the inset of Fig. 3, revealing that the major noise from pump-induced parametric fluorescence was almost eliminated in our experiment. The peak at 0.49 and 0.78 μm represented the second harmonic generation of the pump laser diode for the EDFA at 0.98 μm and the EDFA output at 1.56 μm, respectively. The other peaks were related to the fluorescence of the Er-doped fiber. Considering the pulsed pump mode, the noise was localized within a very narrow time window of the pulsed pump which worked as a coincidence detection gate much shorter than any electronic gates applied on the APD, leading to a very low noise counts on the APD. The single-photon counting of the SPCM as a function of the pump power is shown in Fig. 4. The maximum photon counting of 5.5×10^{5} s^{-1} achieved at the pump power of 59.3 mW, and accordingly the maximum overall

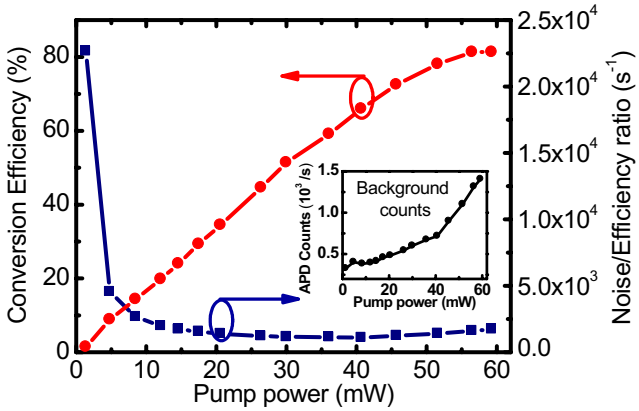

FIG. 4. (Color online) SFG counts (circles) and background counts over conversion efficiency ratio (squares) recorded by the Si-APD SPCM as a function of the pump power. Inset: background counts dependent on the pump power.

detection efficiency η_A was 27.5%. Considering the transmittance of the filters and the quantum efficiency of the SPCM, the maximum conversion efficiency η_c of the system was calculated to be 81.1% by $\eta_A = \eta_C \eta_T \eta_D$ with the corresponding background counts of 1.5×10^3 s^{-1}. As shown in Fig. 4, the increase of the conversion efficiency (in red) became flattened as the pump power increased. It is foreseeable that with the pump power further increased, the periodical oscillation of the conversion efficiency dependent on the pump power would appear. The inset of the Fig. 4 illustrates the background counts as a quadratic function of the pump power, indicating that noise photons might come from the pump-induced hyper-parametric fluorescence, where one noise photon involved two pump photons. Although the background counts increased nonlinearly, it still remained at a very low level. Therefore, with the detection efficiency increasing the noise/efficiency ratio was decreased sharply then kept at a low level as shown in Fig. 4. The photons produced by the spontaneous parametric down-conversion from the longer wavelength pump (1.56 μm) did not appear at the wavelength of the signal photons (1.04 μm). Hence, in this longer-wavelength pump system, we could eliminate the major noise source from the fake background counts at the sum-frequency wavelength mainly originated from frequency upconversion of the parametric fluorescence around the signal wavelength.

In conclusion, efficient infrared single-photon frequency upconversion was demonstrated by frequency upconverting the pulsed single photons with a well-designed synchronous pulsed pump. The maximum conversion efficiency reached about 81.1% with the corresponding background counts of 1.5×10^3 s^{-1}. The quadratic dependence of the background counts on the pump power indicates that the small noise photons might come from the pump-induced hyper-parametric fluorescence. Such a synchronous single-photon frequency upconversion detection system may stimulate promising applications with compact all-fiber devices in temporal and spectral control of single-photon nonlinear photonics.

This work was funded in part by National Natural Science Fund of China (Grant Nos. 10990101, 10525416, 10774045, and 60907043) and National Key Project for Basic Research (Grant No. 2006CB921105).

[1] O. Kuzucu, F. N. C. Wong, S. Kurimura, and S. Tovstong, Opt. Lett. **33**, 2257 (2008).
[2] R. T. Thew, H. Zbinden, and N. Gisin, Appl. Phys. Lett. **93**, 071104 (2008).
[3] R. T. Thew, S. Tanzilli, L. Krainer, S. C. Zeller, A. Rochas, I. Rech, S. Cova, H. Zbinden, and N. Gisin, New J. Phys. **8**, 32 (2006).
[4] M. A. Albota and F. N. C. Wong, Opt. Lett. **29**, 1449 (2004).
[5] K. Wilson and M. Enoch, IEEE Commun. Mag. **38**, 134 (2000).
[6] H. Yamazaki, S. Kaminaka, E. Kohda, M. Mukai, and H. Hamaguchi, Radiat. Med. **21**, 1 (2003).
[7] Q. Zhang, C. Langrock, M. M. Fejer, and Y. Yamamoto, Opt. Express **16**, 19557 (2008).
[8] H. Dong, H. Pan, Y. Li, E. Wu, and H. Zeng, Appl. Phys. Lett. **93**, 071101 (2008).
[9] M. Rusu, R. Herda, and O. G. Okhotnikov, Opt. Express **12**, 4719 (2004).
[10] R. K. Shelton, S. M. Foreman, L. Ma, J. L. Hall, H. C. Kapteyn, M. M. Murnane, M. Notcutt, and J. Ye, Opt. Lett. **27**, 312 (2002).